NASA Technical Paper 1181

Experimental and Analytical Study of Nitric Oxide Formation During Combustion of Propane in a Jet-Stirred Combustor

N. T. Wakelyn, Casimir J. Jachimowski,
and Charles H. Wilson
Langley Research Center
Hampton, Virginia

National Aeronautics
and Space Administration

**Scientific and Technical
Information Office**

1978

SUMMARY

A jet-stirred combustor, constructed of castable zirconia and with an inconel injector, has been used to study nitric oxide formation in propane-air combustion with residence times in the range from 3.2 to 3.3 msec and equivalence ratios varying from 0.7 to 1.4. The residence time range was characteristic of that found in the primary zones of aircraft turbines.

Premixed propane-air formulations were subjected to intense and turbulent backmixed combustion within the cavity formed between the injector and the hemispherical inner walls of the zirconia shell. The volume of the combustor cavity was 12.7 cm^3 and the mass loading was maintained in the range from 0.053 to 0.055 g/cm^3-sec. Measurements were made of combustor operating temperature and of nitric oxide concentration. Maximum nitric oxide concentrations of the order of 55 ppm were found in the range of equivalence ratio from 1.0 to 1.1.

Nitric oxide concentrations were predicted over the range of equivalence ratio by a computer program which employs a perfectly stirred reactor (PSR) algorithm with finite-rate kinetics. A finite-rate chemical kinetic mechanism for propane combustion and nitric oxide formation was assembled by coupling an existing propane oxidation mechanism with the Zeldovich reactions and reactions of molecular nitrogen with hydrocarbon fragments. Analytical studies using this mechanism under simulated experimental conditions revealed that the hydrocarbon-fragment—nitrogen reactions play a significant role in nitric oxide formation during fuel-rich combustion. Good agreement between predicted and measured nitric oxide levels was obtained by adjusting the rate coefficient for the reaction, $CH + N_2 \rightarrow HCN + N$. The kinetic model also predicted quite well the nitric oxide levels measured in experiments with propane-air mixtures in a premixed, prevaporized combustor operating under turbojet conditions.

INTRODUCTION

The ability to model successfully the kinetics of hydrocarbon combustion and nitric oxide formation is important to the development of reliable mathematical models of combustion systems such as aircraft gas turbine combustors. The formation of nitric oxide appears to be adequately described only for the more simple reaction systems, such as combustion of CO, H_2, and, perhaps, methane-lean mixtures (refs. 1 and 2). Excess NO has been found in very fuel-rich flames (ref. 3). The two Zeldovich exchange reactions (ref. 4) are usually used to model NO formation. These reactions are

$$O + N_2 \rightarrow NO + N$$

$$N + O_2 \rightarrow NO + O$$

Another reaction commonly used in fuel-rich combustion conditions is

$$N + OH \rightarrow NO + H$$

Nitric oxide production is predicted by these reactions coupled with reactions describing the oxidation of species containing carbon and hydrogen to produce O and OH. Generally, these predictions are quite low compared with measured values for fuel-rich mixtures. In reference 1, computer predictions obtained from chemical models based upon these reactions were more than 90 percent lower than measured values. Also, pyrolysis of the more complex hydrocarbon fuels produces carbon-hydrogen fragments which appear to complicate the reaction system, so that the Zeldovich mechanism no longer predicts NO formation correctly.

Actually, NO is produced by relatively minor reactions in relation to reactions involved in the combustion process. Since predictions fall short as the concentration of hydrocarbons increases, it is reasonable to assume that carbon-hydrogen fragments are involved in the conversion of N_2 to nitrogen compounds capable of further conversion to NO. The interaction of various carbon and carbon-hydrogen species with atmospheric nitrogen to yield the cyano radical and hydrogen cyanide has been proposed in reference 5 as an explanation of the "prompt" (other than Zeldovich) NO. Experimental confirmation of the presence of CN was presented at the same time (comment on ref. 5). A variety of experimenters (refs. 3, 6, 7, and 8) have detected HCN produced in fuel-rich combustion by reactions involving atmospheric N_2. A stirred-combustor computer model of methane-air combustion (ref. 9) has shown the utility of reactions of the type presented in reference 5. Reactions involving additional species, such as NCO and NH, in the formation of NO have been suggested (refs. 7, 8, 10, 11, and 12), and rate data for a variety of N-C-H-O reactions of this type are presented in reference 13.

The intention of the present study is to test various mechanistic schemes for the prediction of NO formation in propane-air combustion against measured data over a range of fuel-air equivalence ratio from lean to rich and at an applicable mass loading. The data were taken from a laboratory combustion device which employs intensely turbulent backmixing and operates in the millisecond residence-time range, the same range found in the primary zones of aircraft turbines. The device used is a jet-stirred combustor, which has been the object of much development (refs. 1, 14, 15, 16, 17, 18, and 19) over the past 2 decades and which is capable, under certain conditions, of kinetically controlled operation. The computer program used employs the perfectly stirred reactor (PSR) algorithm (ref. 20) which is applicable to certain modes of operation of a suitably designed stirred combustor (ref. 21). The measured data were temperature and NO concentration within the combustion cavity as a function of equivalence ratio.

EXPERIMENTAL APPARATUS AND PROCEDURE

Jet-Stirred Combustor

The combustion device used in the present study is hemispherical in contrast to the spherical geometry of the device used in early stirred-combustor literature (refs. 14, 15, 16, and 17). It is very similar to the combustor used in reference 1, the differences being the shell material and the size of the injector. The body of the combustor was fabricated of castable zirconia with an investment-cast inconel injector, as shown in figure 1. The 1.905-cm-diameter

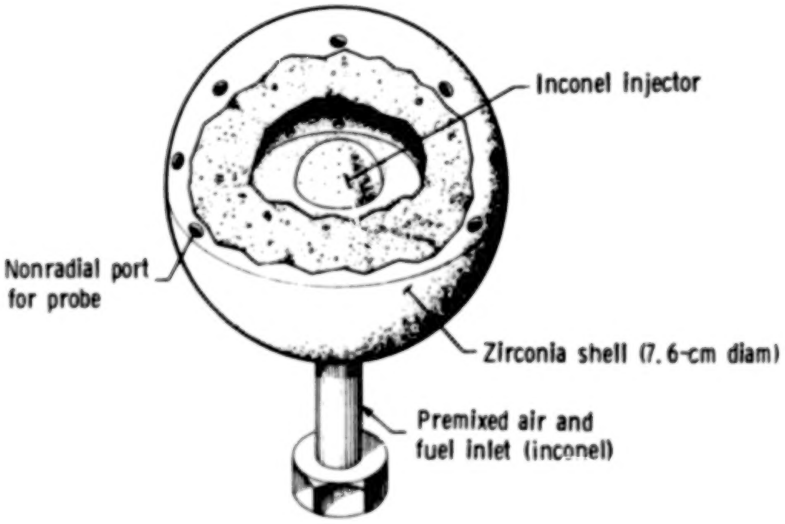

Figure 1.- Drawing of jet-stirred combustor.

spherical inconel injector, formed with a section of inconel tube to which stainless-steel tubing was later welded, was precision drilled to produce 40, 0.0508-cm-diameter radial holes for the injection of combustible mixtures into the 12.7-cm^3 cavity formed between the injector and the outer zirconia shell. The hole placement was essentially a centered hexagonal pattern for several repeat units followed by measured placement to achieve as equidistant a hole distribution as possible. For the exiting of combustion products, the zirconia shell was provided with 25, 0.318-cm-diameter radial holes, spaced so that the streams from the injector impinge upon the shell near the centers of triplets of outside ports. The shell contains two other ports, 0.476 cm in diameter, for insertion of instrument probes. These ports are nonradial and are plugged when not in use. The shell also is cast with three thermocouple ports of varying depths, so that platinum-platinum+14-percent-rhodium thermocouples can be potted therein at the following distances from the center of the injector sphere: 2.14, 2.50, and 3.41 cm. The distance to the outside surface of the shell is 3.8 cm and a thermocouple is also attached at this point.

The nonradial holes in the zirconia shell are larger than the radial exhaust holes to accommodate a gas sampling probe. This water-cooled, stainless steel probe is similar in construction to that of reference 14 but has a 0.013-cm-diameter orifice affixed to its tip. A temperature probe using an iridium-iridium+40-percent-rhodium thermocouple is also used through the nonradial holes. Either probe, depending upon the type of measurement desired, is mounted to a traversing block which is coupled to a linear potentiometer so that the combustion cavity may be scanned at accurate and reproducible depths.

With mass loading fixed in the range from 0.053 to 0.055 g/cm^3-sec corresponding to a mechanistically coupled residence time of 3.25 ± 0.05 msec, equivalence ratio was varied from 0.7 to 1.4. Air and propane rotameters, calibrated against a standard volume and continuously corrected for pressure and temperature, were employed to establish the volumetric mass flow per second.

Gas Temperature

The traversing iridium-iridium+40-percent-rhodium thermocouple, used to record temperatures in a normal scan across the combustor cavity, shifted its millivolt calibration toward a higher temperature indication after being above 1200 K for a time. It was found that wire preannealed at 1273 K for at least 15 minutes would not shift in calibration during a scanning traverse of the combustor cavity. Thermocouples of this type survive prolonged contact with combustion products at about 2000 K.

The 40-percent-rhodium material was used because loss of iridium from the alloyed wire has been observed (ref. 22, pp. 10-11). It was thought that the higher percentage iridium material would be longer lasting in a combustion cavity. Although no X-ray diffraction analysis was performed, it is believed that the calibration shift is due to a solid-state transition rather than to loss of iridium, since the shift appears to be in one step as opposed to being progressive. No intermediate calibrations were obtained.

Platinum-platinum+14-percent-rhodium thermocouples were also used in preliminary measurements within the combustor cavity. Failure of this wire in the vicinity of the injector was often observed. This observation is in accord with early experiments in ignition using a heated platinum loop. The loop, heated to yellow heat, could be maintained within the cavity for prolonged periods of time with flowing air. It would immediately burn open upon entry of propane. It seems that platinum thermocouples would not be preferred where they could come in contact with propane and/or its pyrolyzed derivatives. Even without failure, the temperature indication would be suspect and perhaps liable to catalytic error. Temperature profiles from normal traverses of the combustor cavity for various mass loadings (bracketing those used in this study) are shown in figure 2. The essentially constant temperature over a major portion of the combustor cavity, as shown in the figure, is an indication of homogeneity and thus, a well-mixed operating condition.

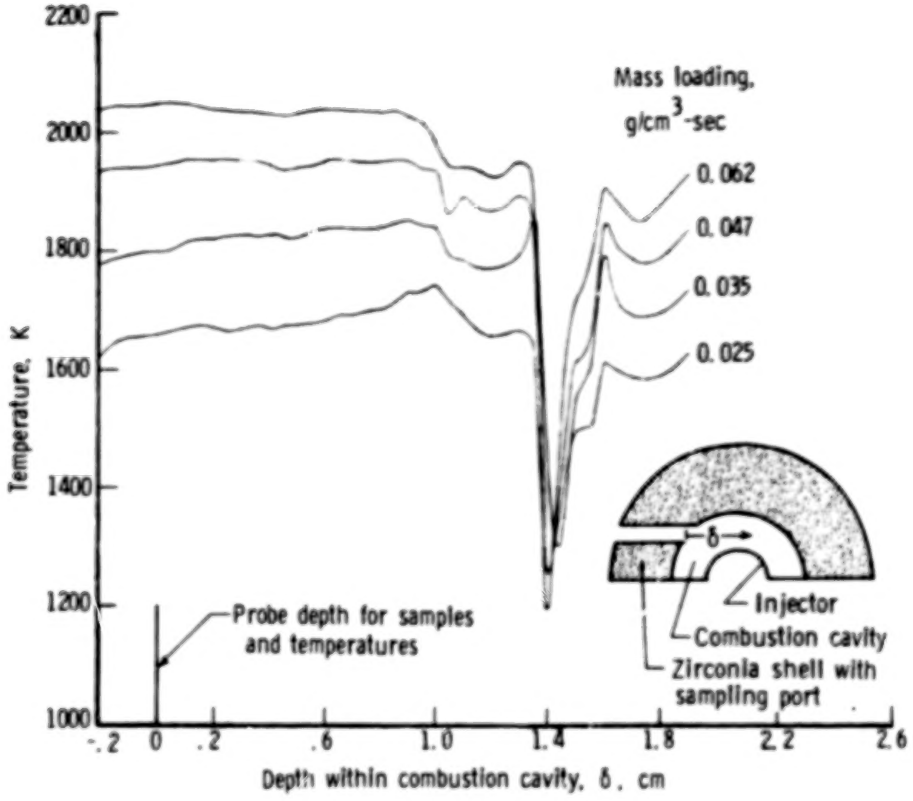

Figure 2.- Temperature profiles from a normal traverse of combustor cavity for various mass loadings.

NO Concentration Measurements

Samples of combustion gases were extracted from the combustor by means of the stainless-steel, water-cooled, gas sampling probe, which was operated as an aerodynamic probe. (See ref. 23.) Samples were taken within the combustor at a depth of 2.15 cm from the outside wall, which encompassed the hottest regions of the flame as determined by temperature traverses across the reaction zone. A diaphragm pump was used to provide a quenched sample flow and to deliver the samples to a chemiluminescent (nitric oxide plus ozone) analyzer for NO concentration measurements. The quenched condition of the sample in the probe was monitored by a pressure transducer in the sampling line close to the probe. Quenched flow at the probe inlet was ensured by maintaining an absolute pressure of 48.3 kPa or less, while pressures within the combustor were always greater than 101.3 kPa (1 atm). (See ref. 24.) Wherever possible, all surfaces (lines, fittings, etc.) in contact with the sample between the combustor and the analyzer consisted of stainless steel and Teflon.[1] (See ref. 25.)

---

[1]Teflon: Registered trademark of E. I. du Pont de Nemours & Co., Inc.

Samples collected for NO analysis were diluted with nitrogen at a ratio of at least 6:1 (five parts nitrogen to one part sample) prior to entering the chemiluminescent analyzer (ref. 25). The dilution was fixed at the beginning of each sampling and was maintained by controlling the nitrogen diluent flow through calibrated linear mass flowmeters with a fine-metering valve in the diluent supply line. The diluent nitrogen contained less than 0.007 ppm NO_x. The objective of diluting the sample with nitrogen was to prevent condensation of water vapor during sample collection and transfer; this would otherwise result both in loss from the sample of nitric oxide and in operational difficulties with the chemiluminescent analyzer. (See ref. 24.)

Before and after collecting each sample for analysis, the analyzer was calibrated by introducing a calibration gas upstream of the pump at a flow rate approximating the sampling rate and diluted 6:1 by the nitrogen diluent. The vendor certified the calibration gas to be 51.4 ppm NO in N_2. Calibration was achieved once the analyzer indicated no drift in its response to NO, which indicated that the NO in the sample had equilibrated within the transfer lines. Actual NO concentrations within the samples were calculated by adjusting the actual readings to reflect the instrument calibrations and the dilution of the collected sample.

COMPUTER PROGRAM

The computer program used makes predictive calculations describing chemically rate-limited homogeneous combustion in a perfectly stirred reactor (PSR) in steady-state operation. The program is basically a combination of the equilibrium program of reference 26 and the PSR solution algorithm of reference 20. It is described in detail in references 21 and 27 and is capable of obtaining solutions at desired mass loadings and equivalence ratios.

The PSR solution algorithm expresses the idea that a fuel-air mixture enters a known volume (combustion chamber) and is instantaneously mixed with reactor contents at constant pressure. Steady-state operation is achieved by concurrent and equivalent outflow of reactants and products. The species concentration within the reacting volume is determined from the balance between the net rate of production (or consumption) of each species by chemical reaction and the difference between the input and output flow rates of the species. A PSR is treated mathematically by formulating the equations for mass, species, and energy conservation as described in reference 20 and solving a system of simultaneous nonlinear algebraic equations.

In essence, the conservation equations for a PSR are formulated by considering a stirred reactor of volume V containing combustion gases at a uniform pressure p and a uniform temperature T. For steady-state operation, conservation of mass is given by

$$\dot{m}^* = \dot{m}$$

where $\dot{m}^*$ is the mass flow rate into the reactor and $\dot{m}$ is the mass flow rate out of the reactor. The superscript * always refers to incoming reactants. Conservation of species is given by

$$\frac{\dot{m}}{V}\left(\sigma_i - \sigma_i^*\right) = W_i \qquad (i = 1,2,3,\ldots,N)$$

where σ_i^* and σ_i are the input and output concentrations of species i, N is the total number of species, and W_i is the rate of formation of species i per unit volume because of chemical reactions. Conservation of energy is given by

$$\sum_{i=1}^{N} \sigma_i^* H_i^* - \sum_{i=1}^{N} \sigma_i H_i = Q$$

where H_i is the enthalpy of species i and Q is the heat loss from the reactor per unit mass because of radiation, thermal diffusion, and convection. For adiabatic operation, of course, Q is zero.

Programs of this type (i.e., for solving problems involving concentration changes with associated energy changes) need a source of thermodynamic data. It was found that the JANAF tables (ref. 28) up to the present time do not contain the data for propane and for some of the complex hydrocarbon species used in some mechanisms. A source of such data has been found (ref. 29) and curve fits of a form suitable for the PSR program have been published (ref. 30).

PROPANE-AIR CHEMICAL KINETIC MODEL

The chemical kinetic reaction model and the rate coefficients used in the numerical simulations of the experiment are listed in table I as a function of the reaction temperature T. The rate coefficients selected for these reactions were obtained from the literature whenever possible. (See refs. 7, 10, and 31 to 39.) Reactions (1) to (57) describe the oxidation mechanism of propane. These reactions and rate coefficients, which were derived from shock-tube experiments, provide a quantitative description of the kinetics of oxygen atom formation, the formation of carbon monoxide and carbon dioxide, and the ignition delay times for the propane-oxygen system. Additional details on the mechanism and the shock-tube experiments are given in reference 31.

Reactions (52) to (57) describe the formation of the hydrocarbon fragments CH_2 and CH by the systematic removal of hydrogen atoms by the radicals H, O,

and OH. The rate coefficients for reactions (52) to (54) were assumed to be the same as the rate coefficients for reactions (55) to (57). Since these reactions are very similar, this assumption does not seem to be unreasonable, considering the lack of reliable experimental rate coefficients for reactions (52) to (54). Reactions (58) to (60) describe the formation of nitric oxide and are often referred to as the Zeldovich reaction scheme. Reaction (61), first suggested by Fenimore in reference 5, when coupled with reactions (59) and (60), is believed to be responsible for the high rate of nitric oxide production that has been observed during combustion of fuel-rich hydrocarbon-air mixtures. The hydrogen cyanide produced through reaction (61) can also be oxidized to nitric oxide. Reactions (62) to (70) describe this oxidation process. The rate coefficient for reaction (69) was estimated to be similar to the rate coefficients for reactions (67) and (68). Since substantial amounts of carbon dioxide are produced during fuel-rich combustion (although the maximum is produced under stoichiometric conditions), it was believed that reaction (71), a very exothermic process, should be included in the model because it could be an important path for CH radical destruction that competes with reaction (61). Since an experimental rate coefficient was not available for reaction (71), the rate coefficient for reaction (65), an analogous process, was used.

RESULTS AND DISCUSSION

Comparison Between Experimental Results and Kinetic Model

Results of the propane-air experiments are assembled in table II and plotted in figures 3 and 4, where the measured reaction temperature and nitric oxide concentration in parts per million are plotted against the fuel-air equivalence ratio. The data were obtained at mass loadings between 0.053 and 0.055 g/cm^3-sec which corresponded to residence times between 3.2 and 3.0 msec. Maximum nitric oxide concentrations of the order of 55 ppm were found in the range of equivalence ratio from 1.0 to 1.1.

To determine the ability of the proposed propane combustion mechanism to predict the experimentally measured nitric oxide levels, computer simulations of the stirred combustor experiments were performed by using the reactions and rate coefficients listed in table I. These simulations were made for fuel-air equivalence ratios of 0.7, 0.8, 1.0, 1.2, 1.3, and 1.4. The heat loss parameter Q was adjusted in these simulations to provide reasonable agreement between the calculated and measured reaction temperatures for a mass loading of 0.054 g/cm^3-sec. The results of these simulations are plotted in figures 3 and 4. The agreement between the calculated and measured nitric oxide levels is very good for the fuel-lean simulation but becomes poorer as the equivalence ratio increases. However, the agreement cannot be considered totally unsatisfactory because the predicted nitric oxide level at an equivalence ratio of 1.3 is only 35 percent lower than the measured value. This difference, however, suggests that the proposed chemical kinetic model, while suitable for nitric

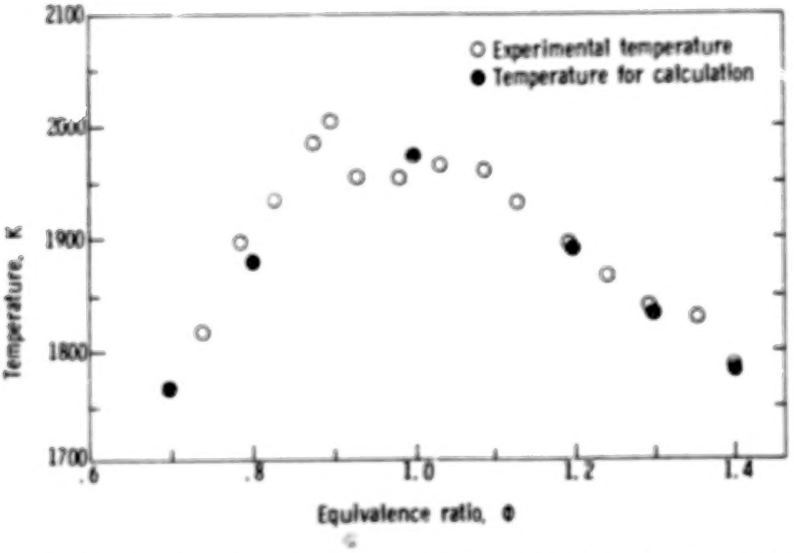

Figure 3.- Temperatures of propane-air mixtures in jet-stirred combustor.

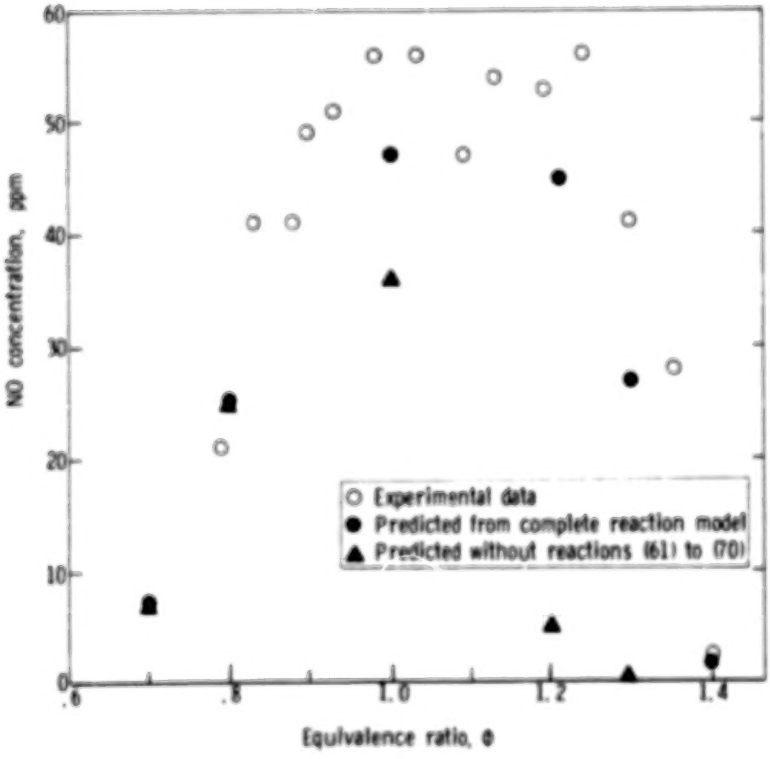

Figure 4.- Comparison between experimental and predicted nitric oxide levels in jet-stirred combustor for propane-air mixtures.

oxide predictions in fuel-lean systems, does need to be improved for fuel-rich nitric oxide predictions.

To better understand the kinetics of nitric oxide formation during fuel-rich combustion, a parametric study was performed in which the rates of reactions (61) to (71) were individually varied and the effect on nitric oxide levels was noted. As anticipated, the rate of reaction (61) had the largest influence on the predicted levels. By increasing the rate coefficient for reaction (61) by a factor of 2, the kinetic model overpredicted the measured nitric oxide levels for equivalence ratios of 1.0, 1.2, 1.3, and 1.4. The parametric study also revealed that the rate of reaction (71) influences the predicted nitric oxide levels, but the effect is not as great as that of reaction (61). Reaction (71) influences nitric oxide production by controlling the CH radical concentration which in turn controls the rate of reaction (61). The rates of reactions (62) to (70) have a much smaller effect on the nitric oxide production rate compared with the effects of reactions (61) and (71).

Results of the parametric study also revealed that the effect of reactions (61) to (71) on nitric oxide production becomes less as the amount of oxygen increases (the equivalence ratio becomes smaller) because reactions (27), (28), and (29) become more important and begin to consume the CH_2 and CH radicals. This effect is illustrated in figure 4 where a comparison is made between the data listed in table II, predictions from the chemical kinetic model listed in table I, and predictions from the same model without reactions (61) to (70). At an equivalence ratio of 0.8, the predicted nitric oxide levels are identical, indicating that the CH and CH_2 radicals are being totally consumed by reactions (27) to (29). The nitric oxide formed in this fuel-lean mixture is essentially produced through the Zeldovich reactions (58) to (60). As the equivalence ratio increases, the contribution of reactions (61) to (71) to nitric oxide production increases, and at an equivalence ratio of 1.3, the contribution of reaction (58) is negligible.

Since the rate of reaction (61) has the largest effect on fuel-rich nitric oxide formation, an attempt was made to adjust the rate coefficient for this reaction to obtain better agreement between the predicted and measured nitric oxide levels. The best agreement was obtained by using the rate coefficient expression, $2.5 \times 10^{11} \exp(-9562/T)$ cm^3/mole-sec. This is 50 percent larger than the original value and certainly within the experimental uncertainty associated with this rate coefficient. The nitric oxide levels predicted by the model using the adjusted rate coefficient are compared with the experimental data in figure 5.

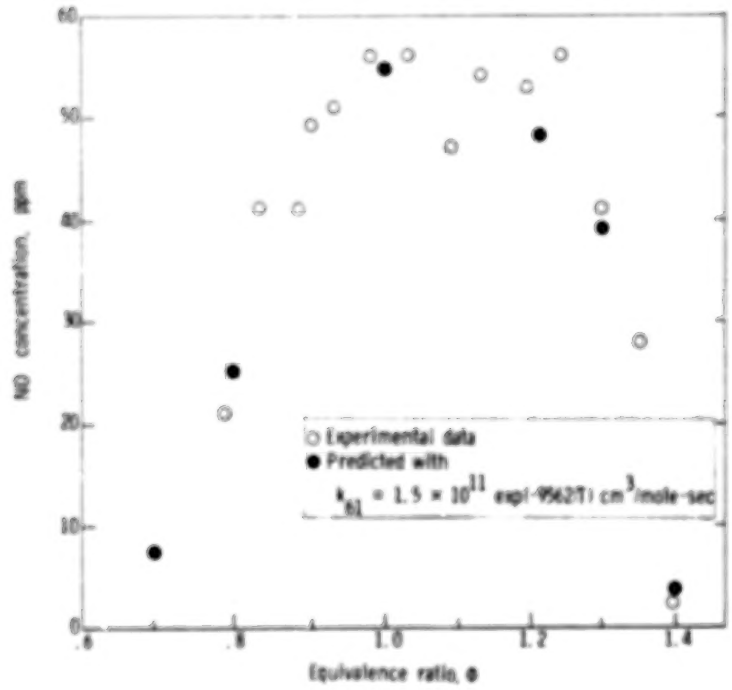

Figure 5.- Experimental nitric oxide levels for propane-air mixtures in jet-stirred combustor compared with those calculated with modified rate coefficient k_{61} for reaction (61).

Application to Other Combustion Systems

One concept that is being investigated for reducing nitric oxide emissions from aircraft gas turbine combustors is the premixed, prevaporized combustor. In the conventional gas turbine combustor, liquid fuel is sprayed directly into the primary zone of the combustor to give a near-stoichiometric mean fuel-air ratio which results in large quantities of nitric oxide being produced. For a premixed, prevaporized fuel system, on the other hand, the fuel-air ratio may be made uniform throughout the primary zone. By operating the combustor at very low equivalence ratios, it is possible to reduce nitric oxide emissions substantially.

Studies on the effect of premixing on nitric oxide emissions (measured as NO_x and reported in equivalent NO_2) for conditions applicable to turbojet combustion have been carried out at NASA Lewis Research Center (refs. 40 and 41). These studies were performed in a 10-cm-diameter flame-tube-type combustor burning premixed gaseous propane fuel. The results of these experiments, given in figure 6, show the strong dependence on equivalence ratio that can be expected from premixed, prevaporized operation. The nitric oxide levels predicted by the chemical kinetic model assembled in this paper are also presented in figure 6. These calculated and measured nitric oxide levels agree quite well.

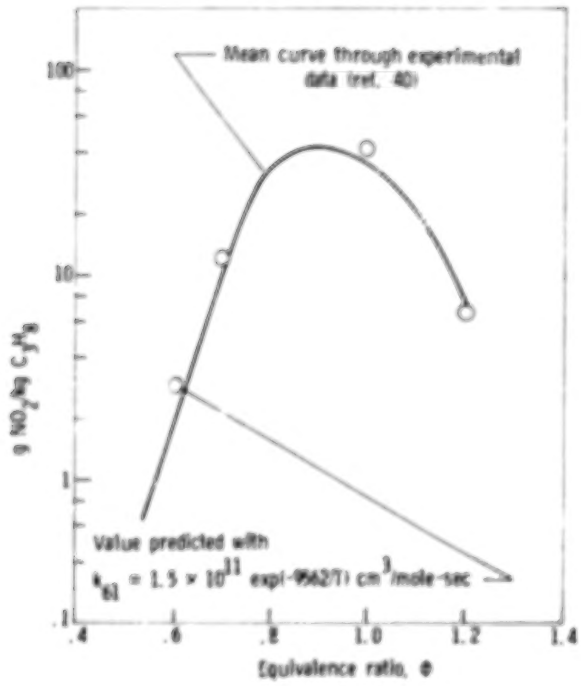

(a) Inlet conditions: 590 K and 5.5 atm.

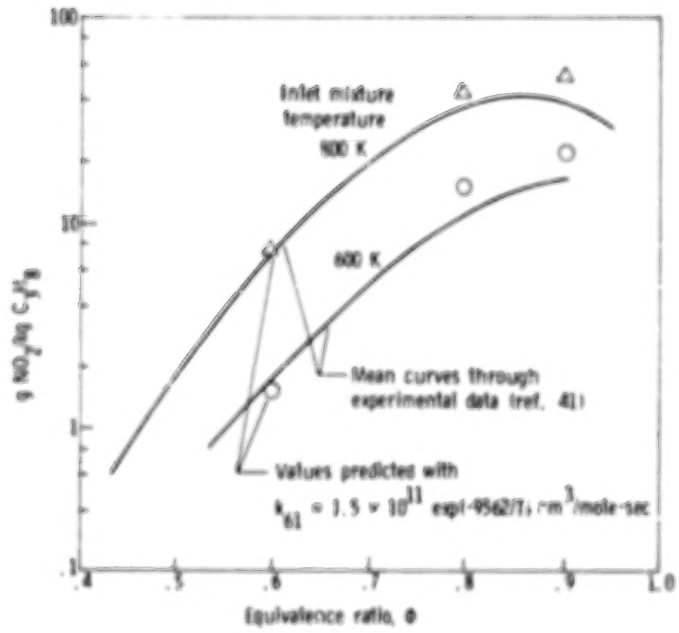

(b) At 5.5 atm and residence time of 2 msec.

Figure 6.- Experimental nitrogen oxide levels for propane-air mixtures in a flame tube-type combustor compared with those predicted with modified rate coefficient k_{61} for reaction (61).

CONCLUDING REMARKS

The purpose of the present study was to test the ability of various reaction steps of a chemical model to predict measured nitric oxide concentrations from a jet-stirred combustor experiment. Computer predictions from a chemical kinetic mechanism for propane-air combustion coupled only with Zeldovich chemistry agreed with experimental results quite well for fuel-lean combustion. For stoichiometric and fuel-rich combustion, the model predictions were quite low in comparison. With the addition of 11 reactions involving reaction of CH with N_2 to produce HCN, oxidation of HCN by O and OH, and the participation of CN, NCO, and NH, stoichiometric and fuel-rich combustion was better described, the predicted nitric oxide level being only 35 percent lower than that measured at an equivalence ratio of 1.3. The preexponential of the reaction $CH + N_2 \rightarrow HCN + N$ was increased by 50 percent (certainly within the experimental uncertainty associated with this rate coefficient) to obtain better agreement. Using this increased rate coefficient and the other 10 reactions without modification provided much better agreement with the experimental data, over the entire range of fuel-air mixtures. The ability of the model to predict reasonably well the nitric oxide levels observed in premixed, prevaporized flame-tube-type experiments suggests that the model is also applicable to other combustion systems.

Langley Research Center
National Aeronautics and Space Administration
Hampton, VA 23665
March 14, 1978

REFERENCES

1. Engleman, V. S.; Bartok, W.; Longwell, J. P.; and Edelman, R. B.: Experimental and Theoretical Studies of NO_x Formation in a Jet-Stirred Combustor. Fourteenth Symposium (International) on Combustion, Combustion Inst., 1973, pp. 755-765.

2. Pratt, David T.; and Malte, Philip C.: Formation of Thermal and Prompt Nitrogen Oxide (NO_x) in a Jet-Stirred Combustor. AIChE Sym. Ser., vol. 71, no. 148, 1975, pp. 150-157.

3. Eberius, K. H.; and Just, Th.: NO Formation in Fuel Rich Flames: A Study of the Influence of the Hydrocarbon Structure. Atmospheric Pollution by Aircraft Engines, AGARD CP-125, Sept. 1973, pp. 16-1 - 16-8.

4. Zel'dovich, Ya. B.: The Oxidation of Nitrogen in Combustion and Explosions. Acta Physicochim., vol. 21, 1946, pp. 577-628.

5. Fenimore, C. P.: Formation of Nitric Oxide in Premixed Hydrocarbon Flames. Thirteenth Symposium (International) on Combustion, Combustion Inst., 1971, pp. 373-379; Comments, pp. 379-380.

6. Bachmaier, F.; Eberius, K. H.; and Just, Th.: The Formation of Nitric Oxide and the Detection of HCN in Premixed Hydrocarbon-Air Flames at 1 Atmosphere. Combust. Sci. & Technol., vol. 7, no. 2, 1973, pp. 77-84.

7. Haynes, B. S.; Iverach, D.; and Kirov, N. Y.: The Behavior of Nitrogen Species in Fuel Rich Hydrocarbon Flames. Fifteenth Symposium (International) on Combustion, Combustion Inst., 1974, pp. 1103-1112.

8. Morley, C.: The Formation and Destruction of Hydrogen Cyanide From Atmospheric and Fuel Nitrogen in Rich Atmospheric-Pressure Flames. Combust. & Flame, vol. 27, no. 2, Oct. 1976, pp. 189-204.

9. Jachimowski, Casimir J.: Analytical Study of Mechanisms for Nitric Oxide Formation During Combustion of Methane in a Jet-Stirred Combustor. NASA TN D-8098, 1975.

10. Mulvihill, Juliet N.; and Phillips, Leon F.: Breakdown of Cyanogen in Fuel-Rich $H_2/N_2/O_2$ Flames. Fifteenth Symposium (International) on Combustion, Combustion Inst., 1974, pp. 1113-1122.

11. Axworthy, A. E.; Schneider, G. R.; Shuman, M. D.; and Dayan, V. H.: Chemistry of Fuel Nitrogen Conversion to Nitrogen Oxides in Combustion. EPA-600/2-76-039, U.S. Environ. Prot. Agency, Feb. 1976.

12. Iverach, David; Kirov, Nikolas Y.; and Haynes, Brian S.: The Formation of Nitric Oxide in Fuel-Rich Flames. Combust. Sci. & Technol., vol. 8, no. 4, 1973, pp. 159-164.

13. Engleman, V. S.; Siminski, V. J.; and Bartok, W.: Mechanism and Kinetics of the Formation of NO_x and Other Combustion Pollutants. Phase II. Modified Combustion. EPA-600/7-76-009b, U.S. Environ. Prot. Agency, Aug. 1976. (Available from NTIS as PB-258 875.)

14. Longwell, John P.; and Weiss, Malcolm A.: High Temperature Reaction Rates in Hydrocarbon Combustion. Ind. & Eng. Chem., vol. 47, no. 8, 1955, pp. 1634-1643.

15. Baker, Marvin Leonard: Combustion in an Intensely Stirred Reactor. Ph. D. Thesis, Massachusetts Inst. Technol., 1956.

16. Nerheim, Noble Martin: The Combustion of Carbon Monoxide in a Well-Stirred Reactor. Ph. D. Thesis, Massachusetts Inst. Technol., 1960.

17. Schneider, George R.: Kinetics of Propane Combustion in a Well Stirred Reactor. Ph. D. Thesis, Massachusetts Inst. Technol., 1960.

18. Miles, Glen Alton: Performance Analysis of the Exothermic, Adiabatic Well Stirred Reactor. Ph. D. Thesis, Massachusetts Inst. Technol., 1964.

19. Morgan, Allan Clark: The Combustion of Methane in a Jet Mixed Reactor. Ph. D. Thesis, Massachusetts Inst. Technol., 1967.

20. Jones, A.; and Prothero, A.: The Solution of the Steady-State Equations for an Adiabatic Stirred Reactor. Combust. & Flame, vol. 12, no. 5, Oct. 1968, pp. 457-464.

21. Pratt, David T.: PSR - A Computer Program for Calculation of Steady-Flow Homogeneous Combustion Reaction Kinetics. Bulletin 336, Washington State Univ.

22. Caldwell, F. R.: Thermocouple Materials. NBS Monogr. 40, U.S. Dep. Commer., Mar. 1, 1962.

23. Tuttle, J. H.; Shisler, R. A.; and Mellor, A. M.: Nitrogen Dioxide Formation in Gas Turbine Engines: Measurements and Measurement Methods. Combust. Sci. & Technol., vol. 9, nos. 5 & 6, 1974, pp. 261-271.

24. Cernansky, N. P.: Sampling and Measuring for NO and NO_2 in Combustion Systems. AIAA Paper No. 76-139, Jan. 1976.

25. Maahs, Howard G.: Interference of Oxygen, Carbon Dioxide, and Water Vapor on the Analysis for Oxides of Nitrogen by Chemiluminescence. NASA TM X-3229, 1975.

26. Gordon, Sanford; and McBride, Bonnie J.: Computer Program for Calculation of Complex Chemical Equilibrium Compositions, Rocket Performance, Incident and Reflected Shocks, and Chapman-Jouguet Detonations. NASA SP-273, 1971.

27. Bowman, Barry Roy: An Analytical and Experimental Study of Nitric Oxide Production in the Primary Zone of a Gas Turbine Combustor. Ph. D. Thesis, Washington State Univ., 1972.

28. JANAF Thermochemical Tables - Second Edition. NSRDS-NBS 37, U.S. Dep. Commer., June 1971.

29. Bahn, Gilbert S.: Approximate Thermochemical Tables for Some C-H and C-H-O Species. NASA CR-2178, 1973.

30. Wakelyn, N. T.; and McLain, Allen G.: Polynomial Coefficients of Thermochemical Data for the C-H-O-N System. NASA TM X-72657, 1975.

31. McLain, Allen G.; and Jachimowski, Casimir J.: Chemical Kinetic Modeling of Propane Oxidation Behind Shock Waves. NASA TN D-8501, 1977.

32. Gay, A.; and Pratt, N. H.: Hydrogen-Oxygen Recombination Measurements in a Shock Tube Steady Expansion. Shock Tube Research. Proceedings of the Eighth International Shock Tube Symposium, J. L. Stollery, A. G. Gaydon, and P. R. Owen, eds., Chapman and Hall Ltd., c.1971, pp. 39/1-39/13.

33. Mayer, S. W.; Schieler, L.; and Johnston, H. S.: Computation of High-Temperature Rate Constants for Biomolecular Reactions of Combustion Products. Eleventh Symposium (International) on Combustion, Combustion Inst., 1967, pp. 837-844.

34. Peeters, Jozef; and Vinckier, Christiaan: Production of Chemi-Ions and Formation of CH and CH_2 Radicals in Methane-Oxygen and Ethylene-Oxygen Flames. Fifteenth Symposium (International) on Combustion, Combustion Inst., 1974, pp. 969-977.

35. Baulch, D. L.; Drysdale, D. D.; Horne, D. G.; and Lloyd, A. C.: Critical Evaluation of Rate Data for Homogeneous, Gas Phase Reactions of Interest in High Temperature Systems. High Temperature Reaction Rate Data, No. 4, Univ. of Leeds (England), Dec. 1969.

36. Jachimowski, Casimir J.: High-Temperature Chemical Kinetic Study of the H_2-CO-CO_2-NO Reaction System. NASA TN D-7897, 1975.

37. Benson, S. W.; Golden, D. M.; Lawrence, R. W.; Shaw, Robert; and Woolfolk, R. W.: Estimating the Kinetics of Combustion Including Reactions Involving Oxides of Nitrogen and Sulfurs. EPA-600/2-75-019, U.S. Environ. Prot. Agency, Aug. 1975.

38. Albers, E. A.; Hoyermann, K.; Schacke, H.; Schmatjko, K. J.; Wagner, H. Gg.; and Wolfrum, J.: Absolute Rate Coefficients for the Reaction of H-Atoms With N_2O and Some Reactions of CH Radicals. Fifteenth Symposium (International) on Combustion, Combustion Inst., 1974, pp. 765-773.

39. Engleman, V. S.; and Bartok, W.: Mechanism and Kinetics of the Formation of NO_x and Other Combustion Pollutants: Phase I. Unmodified Combustion. EPA-600/7-76-009a, U.S. Environ. Prot. Agency, Aug. 1976. (Available from NTIS as PB-258 874.)

40. Anderson, David N.: Effect of Premixing on Nitric Oxide Formation. NASA TM X-68220, 1973.

41. Anderson, David: Effects of Equivalence Ratio and Dwell Time on Exhaust Emissions From an Experimental Premixing Prevaporizing Burner. NASA TM X-71592, 1975.

TABLE I.- PROPANE-AIR REACTION MECHANISM

Reaction	Rate coefficient, k (a)	Reference
(1) $M + C_3H_8 \rightarrow C_2H_5 + CH_3 + M$	$5.00 \times 10^{15} \exp(-32713/T)$	31
(2) $CH_3 + C_3H_8 \rightarrow CH_4 + n\text{-}C_3H_7$	$2.00 \times 10^{13} \exp(-5184/T)$	31
(3) $CH_3 + C_3H_8 \rightarrow CH_4 + i\text{-}C_3H_7$	$2.00 \times 10^{13} \exp(-5184/T)$	31
(4) $H + C_3H_8 \rightarrow H_2 + n\text{-}C_3H_7$	$6.30 \times 10^{13} \exp(-4026/T)$	31
(5) $H + C_3H_8 \rightarrow H_2 + i\text{-}C_3H_7$	$6.30 \times 10^{13} \exp(-4026/T)$	31
(6) $O + C_3H_8 \rightarrow OH + n\text{-}C_3H_7$	$5.00 \times 10^{13} \exp(-5033/T)$	31
(7) $O + C_3H_8 \rightarrow OH + i\text{-}C_3H_7$	$5.00 \times 10^{13} \exp(-5033/T)$	31
(8) $OH + C_3H_8 \rightarrow H_2O + n\text{-}C_3H_7$	$1.60 \times 10^{14} \exp(-1580/T)$	31
(9) $OH + C_3H_8 \rightarrow H_2O + i\text{-}C_3H_7$	$1.60 \times 10^{14} \exp(-1580/T)$	31
(10) $n\text{-}C_3H_7 \rightarrow C_2H_4 + CH_3$	$4.00 \times 10^{13} \exp(-16658/T)$	31
(11) $i\text{-}C_3H_7 \rightarrow C_2H_4 + CH_3$	$1.00 \times 10^{12} \exp(-17363/T)$	31
(12) $n\text{-}C_3H_7 \rightarrow C_3H_6 + H$	$6.30 \times 10^{13} \exp(-19124/T)$	31
(13) $i\text{-}C_3H_7 \rightarrow C_3H_6 + H$	$2.00 \times 10^{14} \exp(-20785/T)$	31
(14) $O + C_3H_6 \rightarrow CH_2O + C_2H_4$	1.00×10^{13}	31
(15) $C_2H_5 \rightarrow C_2H_4 + H$	$3.16 \times 10^{13} \exp(-20483/T)$	31
(16) $H + C_2H_4 \rightarrow H_2 + C_2H_3$	$1.10 \times 10^{14} \exp(-4278/T)$	31
(17) $O + C_2H_4 \rightarrow CH_2O + CH_2$	$2.50 \times 10^{13} \exp(-2516/T)$	31
(18) $O + C_2H_4 \rightarrow CH_3 + HCO$	$2.26 \times 10^{13} \exp(-1359/T)$	31
(19) $OH + C_2H_4 \rightarrow H_2O + C_2H_3$	$1.00 \times 10^{14} \exp(-1761/T)$	31
(20) $M + C_2H_3 \rightarrow C_2H_2 + H + M$	$3.00 \times 10^{16} \exp(-20382/T)$	31

[a]The units for k are sec^{-1} for unimolecular reactions, $cm^3/mole\text{-}sec$ for bimolecular reactions, and $cm^6/mole^2\text{-}sec$ for termolecular reactions. Subscripts to k correspond to reaction numbers.

TABLE I.- Continued

Reaction	Rate coefficient, k (a)	Reference
(21) $H + C_2H_2 \rightarrow H_2 + C_2H$	$2.00 \times 10^{14} \exp(-9562/T)$	31
(22) $O + C_2H_2 \rightarrow C_2H + OH$	$3.20 \times 10^{15} T^{-0.6} \exp(-8556/T)$	31
(23) $O + C_2H_2 \rightarrow CH_2 + CO$	$5.20 \times 10^{13} \exp(-1862/T)$	31
(24) $OH + C_2H_2 \rightarrow H_2O + C_2H$	$6.00 \times 10^{12} \exp(-3523/T)$	31
(25) $C_2H + O_2 \rightarrow HCO + CO$	$1.00 \times 10^{13} \exp(-3523/T)$	31
(26) $C_2H + O \rightarrow CO + CH$	5.00×10^{13}	31
(27) $CH_2 + O_2 \rightarrow HCO + OH$	$1.00 \times 10^{14} \exp(-1862/T)$	31
(28) $CH + O_2 \rightarrow CO + OH$	$1.35 \times 10^{11} T^{0.67} \exp(-12934/T)$	31
(29) $CH + O_2 \rightarrow HCO + O$	1.00×10^{13}	31
(30) $M + CH_4 \rightarrow CH_3 + H + M$	$4.00 \times 10^{17} \exp(-44500/T)$	31
(31) $H + CH_4 \rightarrow H_2 + CH_3$	$1.26 \times 10^{14} \exp(-5989/T)$	31
(32) $O + CH_4 \rightarrow OH + CH_3$	$2.00 \times 10^{13} \exp(-4640/T)$	31
(33) $OH + CH_4 \rightarrow H_2O + CH_3$	$3.00 \times 10^{13} \exp(-3020/T)$	31
(34) $CH_3 + O_2 \rightarrow CH_2O + OH$	$1.70 \times 10^{12} \exp(-7045/T)$	31
(35) $CH_3 + O \rightarrow CH_2O + H$	$1.30 \times 10^{14} \exp(-1006/T)$	31
(36) $H + CH_2O \rightarrow H_2 + HCO$	2.00×10^{13}	31
(37) $O + CH_2O \rightarrow OH + HCO$	2.00×10^{13}	31
(38) $OH + CH_2O \rightarrow H_2O + HCO$	2.30×10^{13}	31
(39) $H + HCO \rightarrow H_2 + CO$	1.00×10^{14}	31
(40) $O + HCO \rightarrow OH + CO$	1.26×10^{14}	31

[a]The units for k are sec^{-1} for unimolecular reactions, $cm^3/mole\text{-}sec$ for bimolecular reactions, and $cm^6/mole^2\text{-}sec$ for termolecular reactions. Subscripts to k correspond to reaction numbers.

TABLE I.- Continued

Reaction	Rate coefficient, k (a)	Reference
(41) $OH + HCO \rightarrow H_2O + CO$	1.00×10^{14}	31
(42) $M + HCO \rightarrow H + CO + M$	$5.00 \times 10^{14} \exp(-9562/T)$	31
(43) $CO + OH \rightarrow CO_2 + H$	$4.00 \times 10^{12} \exp(-4026/T)$	31
(44) $M + CO + O \rightarrow CO_2 + M$	6.00×10^{13}	31
(45) $H + O_2 \rightarrow OH + O$	$1.22 \times 10^{17} T^{-0.91} \exp(-8369/T)$	31
(46) $O + H_2 \rightarrow OH + H$	$2.07 \times 10^{14} \exp(-6920/T)$	31
(47) $OH + H_2 \rightarrow H_2O + H$	$5.20 \times 10^{13} \exp(-3271/T)$	31
(48) $OH + OH \rightarrow H_2O + O$	$5.50 \times 10^{13} \exp(-3523/T)$	31
(49) $M + O_2 \rightarrow O + O + M$	$2.55 \times 10^{18} T^{-1.0} \exp(-59386/T)$	31
(50) $M + 2H \rightarrow H_2 + M$		32
$M = N_2$	3.80×10^{14}	
$M = H_2O$	2.30×10^{15}	
(51) $M + H + OH \rightarrow H_2O + M$		32
$M = N_2$	1.00×10^{16}	
$M = H_2O$	5.00×10^{16}	
(52) $H + CH_3 \rightarrow H_2 + CH_2$	$k_{52} = k_{55}$	Estimated
(53) $O + CH_3 \rightarrow OH + CH_2$	$k_{53} = k_{56}$	Estimated
(54) $OH + CH_3 \rightarrow H_2O + CH_2$	$k_{54} = k_{57}$	Estimated
(55) $H + CH_2 \rightarrow H_2 + CH$	$2.70 \times 10^{11} T^{0.67} \exp(-12934/T)$	33

[a]The units for k are sec^{-1} for unimolecular reactions, $cm^3/mole\text{-}sec$ for bimolecular reactions, and $cm^6/mole^2\text{-}sec$ for termolecular reactions. Subscripts to k correspond to reaction numbers.

TABLE I.- Concluded

Reaction	Rate coefficient, k [a]	Reference
(56) $O + CH_2 \rightarrow OH + CH$	$1.90 \times 10^{11} T^{0.68} \exp(-12934/T)$	33
(57) $OH + CH_2 \rightarrow H_2O + CH$	$k_{57} = k_{55}$	34
(58) $O + N_2 \rightarrow NO + N$	$1.36 \times 10^{14} \exp(-37947/T)$	35
(59) $N + O_2 \rightarrow NO + O$	$6.40 \times 10^{9} T^{1.0} \exp(-3145/T)$	35
(60) $N + OH \rightarrow NO + H$	4.00×10^{13}	36
(61) $CH + N_2 \rightarrow HCN + N$	[b] $1.00 \times 10^{11} \exp(-9562/T)$	37
(62) $CN + H_2 \rightarrow HCN + H$	$6.00 \times 10^{13} \exp(-2669/T)$	38
(63) $O + HCN \rightarrow OH + CN$	$1.40 \times 10^{11} T^{0.68} \exp(-8506/T)$	33
(64) $OH + HCN \rightarrow CN + H_2O$	$2.00 \times 10^{11} T^{0.6} \exp(-2516/T)$	39
(65) $CN + CO_2 \rightarrow NCO + CO$	3.70×10^{12}	7
(66) $CN + O_2 \rightarrow NCO + O$	$3.20 \times 10^{13} \exp(-505/T)$	38
(67) $H + NCO \rightarrow NH + CO$	2.00×10^{13}	10
(68) $O + NCO \rightarrow NO + CO$	2.00×10^{13}	10
(69) $N + NCO \rightarrow N_2 + CO$	1.00×10^{13}	Estimated
(70) $NH + OH \rightarrow N + H_2O$	$5.00 \times 10^{11} T^{0.5} \exp(-1006/T)$	39
(71) $CH + CO_2 \rightarrow HCO + CO$	$k_{71} = k_{65}$	Estimated

[a]The units for k are sec^{-1} for unimolecular reactions, $cm^3/mole\text{-}sec$ for bimolecular reactions, and $cm^6/mole^2\text{-}sec$ for termolecular reactions. Subscripts to k correspond to reaction numbers.

[b]Better agreement with experimental data was obtained by using $1.5 \times 10^{11} \exp(-9562/T)$ $cm^3/mole\text{-}sec$ for this rate coefficient.

TABLE II.- EXPERIMENTAL DATA FOR PROPANE-AIR MIXTURES

IN JET-STIRRED COMBUSTOR

Equivalence ratio	Temperature, K	NO concentration, ppm
0.74	1817	
.79	1894	21
.83	1933	41
.88	1986	41
.90	2005	49
.93	1954	51
.98	1956	56
1.03	1966	56
1.09	1961	47
1.13	1930	54
1.19	1896	53
1.24	1864	56
1.29	1840	41
1.35	1828	28
1.40	1817	2

1. Report No.	2. Government Accession No.	3. Recipient's Catalog No.
NASA TP-1182		

4. Title and Subtitle	5. Report Date
EXPERIMENTAL AND ANALYTICAL STUDY OF NITRIC OXIDE FORMATION DURING COMBUSTION OF PROPANE IN A JET-STIRRED COMBUSTOR	May 1978
	6. Performing Organization Code
7. Author(s) N. T. Wakelyn, Casimir J. Jachimowski, and Charles H. Wilson	8. Performing Organization Report No. L-12052
	10. Work Unit No. 505-03-23-01
9. Performing Organization Name and Address NASA Langley Research Center Hampton, VA 23665	11. Contract or Grant No.
	13. Type of Report and Period Covered Technical Paper
12. Sponsoring Agency Name and Address National Aeronautics and Space Administration Washington, DC 20546	14. Sponsoring Agency Code

15. Supplementary Notes

16. Abstract

A jet-stirred combustor, constructed of castable zirconia and with an inconel injector, has been used to study nitric oxide formation in propane-air combustion with residence times in the range from 3.2 to 3.3 msec and equivalence ratios varying from 0.7 to 1.4. Measurements were made of combustor operating temperature and of nitric oxide concentration. Maximum nitric oxide concentrations of the order of 55 ppm were found in the range of equivalence ratio from 1.0 to 1.1. A finite-rate chemical kinetic mechanism for propane combustion and nitric oxide formation was assembled by coupling an existing propane oxidation mechanism with the Zeldovich reactions and reactions of molecular nitrogen with hydrocarbon fragments. Analytical studies using this mechanism in a computer simulation of the experimental conditions revealed that the hydrocarbon-fragment—nitrogen reactions play a significant role in nitric oxide formation during fuel-rich combustion. Good agreement between predicted and measured nitric oxide levels was obtained by using a rate coefficient for the reaction, $CH + N_2 \rightarrow HCN + N$, equal to $1.5 \times 10^{11} \exp(-9562/T)$ cm^3/mole-sec, where T is temperature (kelvin).

17. Key Words (Suggested by Author(s))	18. Distribution Statement
Kinetics Pollution Combustion Reaction mechanism	Unclassified - Unlimited Subject Category 25

19. Security Classif. (of this report)	20. Security Classif. (of this page)	21. No. of Pages	22. Price*
Unclassified	Unclassified	22	$4.00

* For sale by the National Technical Information Service, Springfield, Virginia 22161

NASA-Langley, 1978